Strain and damage monitoring in carbon-nanotube-based composite under cyclic strain

Luigi Vertuccio[1,*], Vittoria Vittoria[1,2], Liberata Guadagno[1], Felice De Santis[1]

[1]Department of Industrial Engineering – DIIn - University of Salerno

Via Giovanni Paolo II 132, 84084 Fisciano (SA), Italy

[2]IMAST S.c.ar.l. - Technological District on Engineering of polymeric and composite Materials and Structures, Piazza Bovio 22, 80133 Napoli, Italy

lvertuccio@unisa.it; vvittoria@unisa.it; lguadagno@unisa.it; fedesantis@unisa.it

Abstract

The resistive behavior of multi-walled carbon nanotube (MWCNT)/epoxy resins, tested under mechanical cycles and different levels of applied strain, was investigated for specimens loaded in axial tension. The surface normalized resistivity is linear with the strain for volume fraction of MWCNTs between 2.96×10^{-4} and 2.97×10^{-3} (0.05 and 0.5% wt/wt). For values lower than 0.05% wt/wt, close to the electrical percolation threshold (EPT) a non-linear behavior was observed. The strain sensitivity, in the range between 0.67 and 4.45, may be specifically modified by controlling the nanotube loading, in fact the sensor sensitivity decreases with increasing the carbon nanotubes amount. Microscale damages resulted directly related to the resistance changes and hence easily detectable in a non-destructive way by means of electrical measurements. In the fatigue tests, the damage is expressed through the presence of a residual resistivity, which increases with the amount of plastic strain accumulated in the matrix.

Keywords

A. Carbon nanotubes

A. Thermosetting resin

B. Electrical properties

D. Mechanical testing

1. Introduction and background

Filled polymer can be designed to have many distinct properties that may be exploited to develop the next generation of sensors. In particular, thermosetting and thermoplastic polymer filled with specific nano-structured particles can be manufactured to have integrated electrical, electromagnetic, and possibly other functionalities that work in synergy to provide a new generation of stimuli-responsive materials. This is a revolutionary approach that should lead to the creation of a new generation of sensors with desired properties and design flexibilities.

In this context the sensors of stress/strain play a predominant role in the civil, mechanical and aeronautic engineering fields, in fact, the importance of online structural health monitoring (SHM) is increasing because natural disasters, environmental effects like temperature changes, impact loading and other deteriorating conditions affect the strength and the serviceability of the structures. To prevent any failure of the critical members in advance, various SHM and/or nondestructive evaluation (NDE) techniques such as acceleration-based modal testing, x-ray inspection and ultrasonic inspection have been widely used [1].

In aeronautic engineering fields the fiber reinforced polymers (FRPs) are structural materials, specifically designed for lightweight constructions, for which extremely high mechanical performances are generally expected [2]. Since the breakage of composite structures often occurs by interfacial delamination and/or matrix cracking, the investigation of reliable methods for the failure detection in FRPs has recently attracted the interest of both the scientific and industrial community. Therefore, experimental techniques for the in situ monitoring of the strain and/or damage behavior of composite structures could represent an important aspect to increase their reliability. Both traditional methods (based on the application of strain gauges and piezoelectrics) and innovative monitoring techniques (i.e. through fiber optics) usually make use of sensors that, placed either inside or outside the structure, are invasive and relatively expensive [3].

A new possible approach to solve such a problem consists in the design and construction of polymeric materials designed with the required properties. Polymeric materials filled with conductive nanofillers such as carbon nanotubes (CNTs) or other carbon nanostructured forms or magnetic nanoparticles show very interesting properties that can be applied in the field of sensing devices.

To date, two types of resistance-type strain sensors have been developed, i.e., CNT buckypaper sensors and sensors made from various polymer composites with different fillers, including SWCNTs, multiwalled carbon nanotubes (MWCNTs) and carbon nanofibers. The advantage of these novel composite sensors, which is of primary importance, is the higher sensitivity compared to conventional strain sensors such as metal-foil strain gauges [4].

Baughman et al. [5] first reported the electromechanical actuation behavior of nanotubes. Inherent coupling of electrical and mechanical properties makes nanotubes excellent candidates for in situ sensors. Recent reports have utilized nanotubes-based materials as electromechanical actuators [6, 7] and in a variety of sensing applications, [8] including mass sensors [9], humidity sensors [10], and strain sensors [11, 12].

Long-term durability and performance of advanced fiber composites are governed by properties of the polymer matrix and the fiber/matrix interface [13].

Using electrical techniques has been established as a non-invasive way to monitor damage in carbon-fiber-reinforced composites under static and dynamic loading conditions [14-17]. This approach does not give much insight into matrix-dominated mechanisms of fracture that affect durability and is not applicable to composites where fibers are non-conducting (such as glass or aramid fibers). Thostenson et al. [18] bypass the problem, in fact they process glass fiber–epoxy composites and utilize multi-walled nanotubes dispersed in the epoxy phase as distributed sensors to evaluate the onset and evolution of damage in advanced fibrous composites.

Another advantage of CNTs is that the resin filled with CNTs reaches the electrical percolation threshold (EPT) with very low percentage of filler. In particular, it was found that the EPT is closely related to chemical nature of the polymeric matrix and the procedure used to disperse the nanofiller inside the polymer [19, 20]. The EPT can be lower than 0.3% wt/wt for polymeric matrix based on epoxy resins or epoxy mixtures [19, 21, 22].

The highest sensitivity in composite type sensor is obtained near the percolation threshold due to the tunnelling effect between adjacent CNTs and decreases with further increase of carbon-nanotube loading [23-25]. This makes the performance of composite sensors highly dependent on processing conditions

and material properties such as CNT volume fraction and conductance, curing temperature, mixing rate and barrier height of polymer matrix [23, 26]. To some extent, the overall performance can be dominated by matrix properties rather than the intrinsic characteristics of CNTs.

In this paper, the resistive behavior of multi-walled carbon nanotubes (CNTs) embedded inside an epoxy matrix based on diglycidyl ether of bisphenol A was investigated for samples loaded in axial tension and in fatigue tests, in which the samples were subjected to increases/decreases of strain, and the synchronism of the resistive response was checked. The dependence of the performance of composite sensor, on CNT volume fraction has been evaluated.

The aim was to put in evidence the dependence of the composite sensor performance on CNT volume fraction, and to quantitatively estimate the minimum concentration of carbon-nanotubes able to impart reproducible sensing properties to the composite. This concentration, (beyond the EPT), can allow to manufacture a sensor which meets some requirements of the sensor such as: high sensibility, reliability and reversible response.

2. Experimental section

2.1 Materials and sample preparation

The epoxy resins diglycidyl ether of bisphenol A (DGEBA), the hardener 4,4 diaminodiphenylsulfone (DDS) were supplied by Aldrich Chemicals. Multi-walled carbon nanotubes, 3100 Grade, (CNTs) were obtained from Nanocyl S.A. The morphological parameters of the MWCNTs has been carried out by high resolution transmission electron microscopy (HR-TEM). Most of MWCNTs show an outer diameter from 10 to 30 nm, but also an outer diameter lower than 10 nm or larger than 80 nm has been observed. Nanotubes length is from hundreds of nm to one mm. Number of walls, varies from 4 to 20 in most nanotubes [27]. The weight ratio between epoxy precursor and DDS was 10/2.85; they were mixed at 120 °C and the fillers powder were added and dispersed with high power ultrasonic probe (*Hielscher* model UP200S-24kHz) for 20 minutes. The mixtures were cured at 150 °C for 1 hour followed by 3 hours at (220 °C). The samples are coded as Epoxy-XCNT, where X is the carbon nanotube concentration, (for example Epoxy-1.0CNT means a concentration of CNTs of 1% wt/wt).

The prepared samples are summarized in the Table 1.

To evaluate the volume fraction of CNTs inside the filled samples, the following equation was used

$$f = \left(w / \rho_{MWCNT} \right) \Big/ \left(w / \rho_{MWCNT} + (1-w) / \rho_{Epoxy} \right) \quad (1)$$

were w is the weight fraction of carbon nanotubes, ρ_{MWCNT} the carbon nanotubes density (2.09 g/cm^3) [28], and ρ_{epoxy} the matrix density (1.237 g/cm^3).

The density of epoxy resin was evaluated by floating method using mixtures of chloroform (ρ=1.481 g/cm^3) and n-hexane (ρ=0.656 g/cm^3). Before density measurement, a part of epoxy resin was dried, in an oven at 50 °C, and allowed to cool to room temperature in a dryer. After density measurement, the epoxy resin was reweighed, to the nearest 0.1 mg, in order to exclude any possible absorption.

2.2 Electrical conductivity and mechanical measurement

In order to characterize the electrical resistance of the samples, a 2-wire method was used, where the voltage was applied by *HP* E3631A 80W Triple Output Power Supply and the current was measured by a *HP* 34401A multimeter. All measurements were performed in direct current (DC) mode, at room temperature. Two copper cables were used as electrodes, they were cemented on the sample surface using silver paint on one side of the specimen. The cables were centered at the mid-span of the silver painted surface of the specimen, at a distance of 10 mm as shown in Fig. 7. The contact resistance was considered negligible, since the measured electrical resistance was in the order of kΩ. The four-probe method could be more accurate, but the two-probe method was used because it is a simpler method to be carried out for the evaluation of the resistance during tensile test, and this method has successfully been applied [29-31].

The surface resistivity ρ_s (in Ω/sq units) was calculated as

$$\rho_s = \frac{R \cdot W}{L} \quad (2)$$

where R is the surface resistance in Ω, W is the electrode length and L is the distance between electrodes.

The volume electrical resistivity was carried out according to Cabot Test Method (CTM) E043 based on ASTM D4496. Two silver paint electrodes located at the sample edges were used. The specimen length was 30 mm with 5 mm long electrodes, leaving an effective span (L) of 10 mm between the silver electrodes, The specimen width was 10 mm and its nominal thickness was 750 μm. In order to minimize surface effects in the measurements, silver paint electrodes were painted completely covering the ends of the specimens. A DC voltage of 25 V was applied between the electrodes and the volume electrical

conductivity (σ_e) was calculated using the measured electrical resistance (R) and the specimen dimensions as

$$\sigma_e = \frac{L}{A \cdot R} \tag{3}$$

where A is the cross-sectional area of the specimen.

In order to investigate the effects of applied tensile strain on surface resistivity, the epoxy composites sample, in rectangular geometry were tested in axial tension. The specimens were 80 mm long, with 10 mm and 2 mm thickness. The displacement was applied to the composite by means of the machine cross-head motion at a speed of 2 kN/min, while the corresponding force was measured by the machine load cell and converted to axial stress (σ). Mechanical strain (ε) was calculated as the machine crosshead displacement normalized by the gage length of the test specimen. Two copper wires were connected on the film surface with silver paint on both sides of the specimen, to act as electrodes. Each sample type was first tested up to failure with the aim of evaluating the strain range corresponding to the elastic and plastic behavior. Tensile tests were performed on the samples using a dynamometric apparatus INSTRON (model 4301).

3 Results and discussion

Surface resistivity and volume conductivity of the rectangular samples was first measured without applying any strain. Fig. 1 shows inverse of surface resistivity, $1/\rho_0$, on the left axis, and volume electrical conductivity, σ_e, on the right axis as a function of the volume fraction of CNTs, where ρ_0 is the initial surface resistivity without load.

It is clear that the dispersion of CNTs into the polymer resin significantly increases the conductivity as expected. In fact, the effect of CNTs on the electrical conductivity of epoxy polymers is well-known in literature [20, 21, 32-45]. The conduction in CNTs composites has been explained by considering that conductive paths, causing the material to convert from an insulator to a conductor, are formed in the composite when the CNT concentration ν increases over a threshold value ν_c. The percolation theory describes the dependence of the conductivity σ on the filler concentration by a scaling law of the form

$$\sigma = \sigma_0 \left(\nu - \nu_c\right)^t \tag{4}$$

where ν_c is the percolation threshold and *t* an exponent depending on the system dimensionality [19, 20, 34-40, 46-48]. In particular, Bauhofer et al. [19], based on a global survey of the data available in the literature, presented some general results concerning a systematic correlation characteristics of materials (polymeric matrices, the CNTs type, method of synthesis, processing, etc.) and parameters which describe the law percolation.

As shown in Fig. 1, the composite exhibit the typical abrupt increase of the conductivity predicted by the percolation theory, with the electrical percolation $f_c \leq 1.48\times10^{-4}$ volume fraction (0.015% wt/wt). The value 6.73×10^{-7} volume fraction of the electric percolation threshold (f_c) was obtained by best fitting of the experimental data with the Eq. 4, shown in terms of the inverse of the surface resistivity and volume fraction in the inset in Fig. 1.

In order to observe a direct relationship between strain and change in surface resistivity, the following normalized quantity, defined as normalized surface resistivity, was introduced:

$$\rho^* = \frac{\rho - \rho_0}{\rho_0} \tag{5}$$

where ρ_0 is the resistivity as previously defined. Finally to quantify this phenomenon, sensitivity factor (*SF*), modeled after that of conventional strain gages (also known as gage factor) was adopted the Eq. (6),

$$SF = \frac{\Delta R}{R_0 \varepsilon} \tag{6}$$

where ΔR is the change in electrical resistance, R_0 is the value of electrical resistance before loading and ε is the measured strain. The mechanical tests were carried out on samples loaded in the range of weight percentages [0.025÷0.5] (see Table 1). In particular, the sample was tested with increasing strain cycles, in which for each elongation was evaluated the electrical resistance. At the end of the electrical measurement the sample was returned to its initial conditions (no load).

Fig. 2 shows the stress-strain behavior cycles for sample Epoxy-0.1CNT. The number of cycles varies for each sample, in fact an increase of the amount of carbon nanotubes leads to a decrease of the strain at break and a lower number of cycles obtained; a similar behavior is found in previous paper [49]. In particular, the sample Epoxy-0.1CNT reaches the maximum around 3.5% wt/wt and then undergoes the break following in the successive cycle (8^{th} cycle, not shown in Fig. 2); the cycles are shifted along the x axis for a better reading of the strain for each cycle. A similar mechanical behavior was observed for samples filled with other CNTs percentages.

Figs. 3 and 4 show a direct relationship between the strain and the change in normalized surface resistivity (ρ*) for all the samples with the weight percentage of CNTs between 0.025 and 0.500; surface resistivity proportionally increases with increasing tensile strain. This can be explained by noting that, for a conductor-filled polymer to be electrically conductive, the filler particles must either touch to form conductive paths, or be sufficiently close to each other to enable conductance via ‘‘tunneling effect’ [50, 51]. Conductivity (or resistivity) of a given polymer/filler system therefore is dictated by the number of contact points and the distances between neighboring particles. Since applied tensile strain likely causes loss of contact and widening of the inter-particle distances, hence reducing the current-carrying ability of conductive network and resulting in higher electrical resistance. A very similar scenario was suggested in a number of studies on carbon black-filled rubber composites, where significant rise in resistivity was observed in samples subjected to high tensile strains, from tens to a few hundred percents [52-54]. It should be noted that, in the case of CNTs, tensile strain could also cause realignment of the CNTs, making the network more conductive after removing tensile load. This effect was explained in several experiments with carbon fiber–polymer composite laminates [55, 56]. However, in the case of CNTs, considering their smaller sizes with respect to carbon fibers, and the weak interaction with the polymeric matrix, a such effect should be dwarfed by the increase in resistivity due to the aforementioned tensile strain-induced disruption of conductive network. In Fig. 3, it is evident that the slope of the curve increases with decreasing CNT loading, indicating that the sample responds more sensitively at a lower carbon-nanotube content. It is worth noting that ρ* shows a linear trend with ε for samples with weight percentage of CNTs between 0.050 and 0.500. A similar behavior was reported by Ku-Herrera and Aviles [30] with carbon/vinyl ester composites and by Njuguna et al. [57] with carbon nanotubes sandwiched epoxy resins. A non-linear behavior was observed by Hu et al. [4, 23] for carbon nanofiller/polymer composite fabricated by in *situ* polymerization. In particular, they report for their formulations a very interesting ultrahigh strain sensitivity [4]. In this last case, the epoxy matrix was obtained by mixing the bisphenol-F epoxy resin and an amine hardener; as nanofiller they used MWCNTs and vapor growth carbon fibers (VGCFs) with nickel, copper and silver coatings. They found an exponential relationship of ρ* with ε. This different trend was explained considering the changes in tunneling resistance and the distance among neighboring CNTs [23, 26, 58-63].

Now, through the data shown in the present paper, we are able to better understand this different behavior for sensors that can rich very high values of strain sensitivity; in fact, for the same epoxy matrix (DGEBA) and nature of the nanofiller (MWCNTs – grade 3100) different trends are observed depending

on the CNT concentration. A nonlinear behavior was obtained for the sample filled with a very low concentration of CNTs (0.025% wt/wt) as it can be seen in Fig. 4.

The reason of this non-linear trend can be understood in light of the previous papers and our results. In fact, data here shown, highlight that a nanofiller concentration very close to the EPT, as the investigated concentration of 0.025% wt/wt (Fig.4), determines a non linear trend because the conductivity is very sensitive to the changes in tunneling resistance and the distance among neighboring CNTs. If we consider this result considering the

conductive network in terms of conductive paths, it is quite obvious that the conductivity changes in a very wide range also when the electrical contacts are destroyed because of the strain for nanofiller concentrations corresponding to the EPT.

As expected, the influence of the electrical contacts and the changes in the tunneling resistance on the conductivity of the nanocomposite is less important beyond the EPT, due to the very high number of electrical contacts or spatial domains able to promote the tunneling effect among neighboring CNTs.

In the case of our sensors, even if the behavior of the sensor under tensile strain has been studied for high values ε of strain, compared to those obtained from Hu et al. (strain<0.6%) [4, 23], the trends are similar, in fact, for high concentrations of nanotubes, the behavior of the resistance change ratio versus the strain is linear, whereas it exponentially increases as the concentration approaches the percolation threshold.

Concluding, the sensitivity obtained by Eq. 6, as shown in Fig. 5, decreases as the content of carbon nanotubes increases. The evaluation of the *SF* of the sample, shown in Fig. 4, was obtained in the first linear section, in other words *SF* was obtained for a strain lower than 1.5%.

A similar behavior has been observed by Park et al. [25]: a semi-empirical model, based on the percolation theory, was developed to identify the relationship between applied strain and sensitivity factor. The model suggested that the sensitivity can be tailored over a broad range by varying MWNT loading, matrix type and sample fabrication method. In particular, Park et al. assert that in highly strain-sensitive material can be obtained when the MWNT loading approaches the percolation threshold.

Tensile tests carried out by increasing the strain proved to be very suitable to identify the potential of the filled systems for the sensing of stresses/strains and occurring damage. Fig. 6 shows exemplary courses of stress and strain over time for the chosen testing procedure; the measurement was performed on the specimens containing 0.05% wt/wt (Fig. 6A) and 0.1% wt/wt (Fig.6B) of CNTs. Each sample was subjected to tensile loading cycles, with increasing strain per cycle. At the end of each cycle, the crosshead returns in the initial position (ε=0). In particular the crosshead displaces at a speed of 1

mm/min up to a predetermined strain, the crosshead remains in this position for 1 minute and then it returns in the initial position in which it remains for 2 minutes. The cycle is repeated in the same conditions for 5 times. The following cycles are repeated at a predetermined strain higher than the previous. The fatigue test carried out up to a failure of sample.

Experiments have been carefully performed: at this purpose the experiments were performed on samples marked in the proximity of the grips, and for all the test no slippage was observed. In particular, the local deformation was detected by recording photographically the displacement of marks [31]. The schematic diagram of a single cycle is shown in Fig. 7.

To verify the reversibility of sensor response in tensile mode, samples were subjected to increases/decreases of strain, and the synchronism of the resistive response was checked (Fig. 8A and Fig. 8B). During the mechanical test, the samples were subjected to constant voltage in order to evaluate the temporal variations of the resistivity. The sample containing 0.05% wt/wt MWCNT presents a number of cycles higher than the sample containing 0.1% wt/wt MWCNTs (see Fig. 6) before the break. The concentration of the nanofiller inclusion influences the strain at break, and in general CNTs inclusion in polymeric matrix always decreases the strain at the break [64].

The resistive response of the sample containing 0.1% wt/wt MWCNTs (Fig. 8A) is regular, in fact, the resistivity variations, at the same value of the strain, show equal values in the ratio $\Delta R/R_0$ (%).It is worth noting that when the strain exceeds the value of 0.47% (after the fifth loading cycle), a residual resistivity is detected occurs for the unloaded sample ($\sigma = 0$). This phenomenon is even more relevant for higher values of strain (see the behavior for ε=1.77%). A similar result was obtained by Böger et al. [65], as they show the correlation of the emerging residual strain after each cycle with the corresponding irreversible resistance change.

Böger et al [65] report that the incremental tensile tests proved to be very suitable to identify the potential of the nanocomposite matrix systems for the sensing of stresses/strains and occurring damage. The samples (conductive nanocomposite epoxy) were subjected to tensile loading cycles, and Böger et al [65] assert that after the fifth loading cycle, some residual strain occurs when the specimen is unloaded to zero stress. This residual strain is increasing with each subsequent loading cycle and can be attributed to plastic matrix deformation and damage occurring.

In our case when the crosshead returns to the initial position, for ε_{max}<0.47%, $\Delta R/R_0$ practically returns to zero after each loading cycle, indicating that significant permanent deformation or irreversible damage has not yet occurred in the composite.

For larger values of $\varepsilon_{max,}$ a large residual value of $\Delta R/R_0$ is observed when ε=0. Such a value of residual $\Delta R/R_0$ will be herein referred as ''permanent'' and labeled $\Delta R_P/R_0$. From Fig. 8A, it is possible to observed that the ratio $\Delta R_P/R_0$ increases with increasing ε_{max} from a value 0.1% to 0.33%. A similar result was observed by Ku-Herrera and Aviles [30], indeed the permanent changes in the electrical resistance of the composite scale with the amount of plastic strain accumulated in the polymer matrix are sensitive to the loading history.

The resistive response of the sample containing 0.05% wt/wt of MWCNT (Fig. 8B) is irregular; in fact for $\varepsilon < 0.7\%$ the resistive response is not well highlighted. Also, for the subsequent deformation, $\Delta R_P/R_0$ does not remain constant with the number of cycles. This can be attributed, most likely, to the uneven distribution of the network of nanotubes. It should be recalled that 0.05% wt/wt is a percentage very close to the percolation threshold, and for this reason also the distribution of the contacts CNT-CNT is not uniform as that obtained for the sample containing 0.1% wt/wt of filler. After stretching, the conductive paths are altered irreversibly, and, when the sample is brought back to zero load, a new path is created that is associated to $\Delta R_p/R_0$. The value of $\Delta R_p/R_0$ does not remain constant, because the path that is created in each cycle differs from the previous. In other words, in order to have a regular and reproducible resistive response during performance of the mechanical cycles, the system must have an amount of CNT-CNT contacts suitable for reproducing the same residual $\Delta R/R_0$. The value $\Delta R/R_0$ as a function of the strain for the samples filled with 0.1% wt/wt and 0.05wt/wt of CNT is shown in Fig. 9. The sample with higher concentration of CNTs shows a linear dependence of $\Delta R/R_0$ with the strain. The composite sensor filled with 0.05% wt/wt of CNT shows higher $\Delta R/R_0$ values (at the same strain level) than the sample with lower amount of CNTs, and an exponential relationship. Böger et al. found a similar behavior [65] for two composites having the same amount of carbon fillers (0.3% wt/wt) but with different nature of the nanofiller (exponential behavior for carbon black, linear behavior for carbon nanotubes). They stated that the carbon black composite with a concentration of 0.3% wt/wt is close to the percolation region and therefore much more sensitive to the applied stress/strain and occurring damage; whereas, the composite containing 0.3% wt/wt of MWCNTs is far above the percolation threshold and therefore exhibits a much more redundant conductive network structure. Thus, the sensitivity of this system vs. damage was lower, compared to the carbon black modified matrix.

In our work the relationship $\Delta R/R_0$ vs ε is determined by the amount of carbon nanotubes, in other words, by the density of conductive pathways.

In particular, Shui and Chung [49] found a similar behavior for a composites having the same amount of carbon fillers (volumetric 7%) but with different size of the filler. They found that, the relationship between $\Delta R/R_0$ and strain, during cyclic loading, of carbon filament PES-matrix composite, is much more linear and less noisy than carbon fiber PES-matrix composite, where PES is polyether sulfone, the carbon fibers and the carbon filaments have diameter 10 μm and 0.15 μm respectively.

In order to explain the phenomenon of electrical conduction in the test cycles, it is possible to consider the filled samples as a system consisting of two conductive paths: a) in the condition of intensive network, where the network consists of a relatively high contact number CNT/CNT, and b) in the condition of sparse network, where it consists of a relatively high contact number CNT/CNT. The effect of strain causes a change in resistance when the sample returns to the initial conditions ($\varepsilon=0$), the irreversible breakage of a contact CNT/CNT occurs and the system shows a residual permanent resistance. In the first situation at the end of each cycle, for each rupture of a conductive path, most likely a new conductive contact occurs, hence the value of $\Delta R_p/R_0$ does not change. In condition of sparse network, however, the rate between [number of broken]/[contact number CNT/CNT] changes for each test cycle. This leads to different values of $\Delta R_P/R_0$ at the end of each cycle.

A similar interpretation is also valid to explain the change in the resistance for the same value of the applied strain (see fig. 8B). Thus, ΔR is constant when the system Epoxy/CNT is characterized by an intensive network, variable when the system is characterized by a sparse network.

4. Conclusions

In this study, the electrical resistance of Epoxy/CNT samples subjected to tensile strains was measured, and the potential applications of the material as strain sensor with a broad range of tunable sensitivity were investigated.

The performed tests have shown that the surface resistivity of the composites increased with the tensile strain. This behavior has been attributed to the reduction of the conductive network density and to an increase of the inter-tube distances induced by the applied strains. The sensor sensitivity was found to decrease with the increase of the carbon nanotube amount. Fatigue tests have shown, after a series of loading cycles, the presence of a residual resistivity when the specimens were unloaded to zero stress. The permanent changes in the electrical resistance of the composite increase with the amount of plastic strain accumulated in the polymer matrix and they are sensitive to the content of the carbon nanotubes.

The reproducibility in the residual resistivity value is obtained only when the CNT content is higher than a “limit concentration” which is beyond the EPT. Values higher than the limit concentration lead to reversible breakages of conductive CNT/CNT contacts occurring in a dynamic equilibrium; on the contrary, no dynamic equilibrium is reached at concentrations lower than the value corresponding to the “limit concentration”.

Acknowledgments The activities were performed in the frame of the project “IMPRESA” (DM60704) granted to IMAST S.c.a.r.l. and funded by the M.I.U.R.

References

[1] Park S, Shin H-H, Yun C-B. Wireless impedance sensor nodes for functions of structural damage identification and sensor self-diagnosis. Smart Materials and Structures. 2009;18(5):055001.

[2] Ashby MF. Materials Selection in Mechanical Design . Elsevier. ISBN 0-7506-6168-2, p 519; 2005.

[3] Staszewski W, Boller C, Tomlinson GR. Health monitoring of aerospace structures: smart sensor technologies and signal processing: Wiley. com; 2004.

[4] Hu N, Itoi T, Akagi T, Kojima T, Xue J, Yan C, et al. Ultrasensitive strain sensors made from metal-coated carbon nanofiller/epoxy composites. Carbon. 2012.

[5] Baughman RH, Cui C, Zakhidov AA, Iqbal Z, Barisci JN, Spinks GM, et al. Carbon nanotube actuators. Science. 1999;284(5418):1340-4.

[6] Ahir SV, Terentjev EM. Photomechanical actuation in polymer–nanotube composites. Nature materials. 2005;4(6):491-5.

[7] Spinks GM, Mottaghitalab V, Bahrami-Samani M, Whitten PG, Wallace GG. Carbon-Nanotube-Reinforced Polyaniline Fibers for High-Strength Artificial Muscles. Advanced materials. 2006;18(5):637-40.

[8] Li C, Chou T-W. Atomistic modeling of carbon nanotube-based mechanical sensors. Journal of intelligent material systems and structures. 2006;17(3):247-54.

[9] Li C, Chou T-W. Mass detection using carbon nanotube-based nanomechanical resonators. Applied Physics Letters. 2004;84(25):5246-8.

[10] Su P-G, Huang L-N. Humidity sensors based on TiO< sub> 2</sub> nanoparticles/polypyrrole composite thin films. Sensors and Actuators B: Chemical. 2007;123(1):501-7.

[11] Dharap P, Li Z, Nagarajaiah S, Barrera E. Nanotube film based on single-wall carbon nanotubes for strain sensing. Nanotechnology. 2004;15(3):379.

[12] Halary J, Cookson P, Stanford JL, Lovell PA, Young RJ. Smart nanostructured polymeric coatings for use as remote optical strain sensors. Advanced Engineering Materials. 2004;6(9):729-33.

[13] Chou T-W. Microstructural design of fiber composites: Cambridge University Press; 2005.

[14] Schulte K, Baron C. Load and failure analyses of CFRP laminates by means of electrical resistivity measurements. Composites Science and Technology. 1989;36(1):63-76.

[15] Weber I, Schwartz P. Monitoring bending fatigue in carbon-fibre/epoxy composite strands: a comparison between mechanical and resistance techniques. Composites Science and Technology. 2001;61(6):849-53.

[16] Kupke M, Schulte K, Schüler R. Non-destructive testing of FRP by dc and ac electrical methods. Composites Science and Technology. 2001;61(6):837-47.

[17] Schueler R, Joshi SP, Schulte K. Damage detection in CFRP by electrical conductivity mapping. Composites Science and Technology. 2001;61(6):921-30.

[18] Thostenson ET, Chou TW. Carbon nanotube networks: sensing of distributed strain and damage for life prediction and self healing. Advanced materials. 2006;18(21):2837-41.

[19] Bauhofer W, Kovacs JZ. A review and analysis of electrical percolation in carbon nanotube polymer composites. Composites Science and Technology. 2009;69(10):1486-98.

[20] Guadagno L, Naddeo C, Vittoria V, Sorrentino A, Vertuccio L, Raimondo M, et al. Cure Behavior and Physical Properties of Epoxy ResinFilled with Multiwalled Carbon Nanotubes. Journal of Nanoscience and Nanotechnology. 2010;10(4):2686-93.
[21] Guadagno L, De Vivo B, Di Bartolomeo A, Lamberti P, Sorrentino A, Tucci V, et al. Effect of functionalization on the thermo-mechanical and electrical behavior of multi-wall carbon nanotube/epoxy composites. Carbon. 2011;49(6):1919-30.
[22] De Vivo B, Guadagno L, Lamberti P, Raimondo M, Spinelli G, Tucci V, et al. Electrical properties of multi-walled carbon nanotube/tetrafunctional epoxy-amine composites. AIP Conference Proceedings2012. p. 199.
[23] Hu N, Karube Y, Arai M, Watanabe T, Yan C, Li Y, et al. Investigation on sensitivity of a polymer/carbon nanotube composite strain sensor. Carbon. 2010;48(3):680-7.
[24] Kang I, Schulz MJ, Kim JH, Shanov V, Shi D. A carbon nanotube strain sensor for structural health monitoring. Smart Materials and Structures. 2006;15(3):737.
[25] Pham GT, Park Y-B, Liang Z, Zhang C, Wang B. Processing and modeling of conductive thermoplastic/carbon nanotube films for strain sensing. Composites Part B: Engineering. 2008;39(1):209-16.
[26] Hu N, Karube Y, Yan C, Masuda Z, Fukunaga H. Tunneling effect in a polymer/carbon nanotube nanocomposite strain sensor. Acta Materialia. 2008;56(13):2929-36.
[27] Guadagno L, Vertuccio L, Sorrentino A, Raimondo M, Naddeo C, Vittoria V, et al. Mechanical and barrier properties of epoxy resin filled with multi-walled carbon nanotubes. Carbon. 2009;47(10):2419-30.
[28] Gojny FH, Wichmann MH, Fiedler B, Kinloch IA, Bauhofer W, Windle AH, et al. Evaluation and identification of electrical and thermal conduction mechanisms in carbon nanotube/epoxy composites. Polymer. 2006;47(6):2036-45.
[29] Oliva-Avilés A, Avilés F, Sosa V. Electrical and piezoresistive properties of multi-walled carbon nanotube/polymer composite films aligned by an electric field. Carbon. 2011;49(9):2989-97.
[30] Ku-Herrera J, Aviles F. Cyclic tension and compression piezoresistivity of carbon nanotube/vinyl ester composites in the elastic and plastic regimes. Carbon. 2012;50(7):2592-8.
[31] De Vivo B, Lamberti P, Spinelli G, Tucci V, Vertuccio L, Vittoria V. Simulation and experimental characterization of polymer/carbon nanotubes composites for strain sensor applications. Journal of Applied Physics. 2014;116(5):054307.
[32] Sandler J, Shaffer M, Prasse T, Bauhofer W, Schulte K, Windle A. Development of a dispersion process for carbon nanotubes in an epoxy matrix and the resulting electrical properties. Polymer. 1999;40(21):5967-71.
[33] Song YS, Youn JR. Influence of dispersion states of carbon nanotubes on physical properties of epoxy nanocomposites. Carbon. 2005;43(7):1378-85.
[34] Martin C, Sandler J, Windle A, Schwarz M-K, Bauhofer W, Schulte K, et al. Electric field-induced aligned multi-wall carbon nanotube networks in epoxy composites. Polymer. 2005;46(3):877-86.
[35] Sandler J, Kirk J, Kinloch I, Shaffer M, Windle A. Ultra-low electrical percolation threshold in carbon-nanotube-epoxy composites. Polymer. 2003;44(19):5893-9.
[36] Moisala A, Li Q, Kinloch I, Windle A. Thermal and electrical conductivity of single-and multi-walled carbon nanotube-epoxy composites. Composites Science and Technology. 2006;66(10):1285-8.
[37] Kovacs JZ, Velagala BS, Schulte K, Bauhofer W. Two percolation thresholds in carbon nanotube epoxy composites. Composites Science and Technology. 2007;67(5):922-8.

[38] Kim YJ, Shin TS, Choi HD, Kwon JH, Chung Y-C, Yoon HG. Electrical conductivity of chemically modified multiwalled carbon nanotube/epoxy composites. Carbon. 2005;43(1):23-30.
[39] Du F, Fischer JE, Winey KI. Effect of nanotube alignment on percolation conductivity in carbon nanotube/polymer composites. Physical Review B. 2005;72(12):121404.
[40] Špitalský Z, Krontiras CA, Georga SN, Galiotis C. Effect of oxidation treatment of multiwalled carbon nanotubes on the mechanical and electrical properties of their epoxy composites. Composites Part A: Applied Science and Manufacturing. 2009;40(6):778-83.
[41] Bryning MB, Islam MF, Kikkawa JM, Yodh AG. Very Low Conductivity Threshold in Bulk Isotropic Single-Walled Carbon Nanotube–Epoxy Composites. Advanced materials. 2005;17(9):1186-91.
[42] Vionnet-Menot S, Grimaldi C, Maeder T, Strässler S, Ryser P. Tunneling-percolation origin of nonuniversality: Theory and experiments. Physical Review B. 2005;71(6):064201.
[43] Mdarhri A, Carmona F, Brosseau C, Delhaes P. Direct current electrical and microwave properties of polymer-multiwalled carbon nanotubes composites. Journal of Applied Physics. 2008;103(5):054303--9.
[44] Barrau S, Demont P, Peigney A, Laurent C, Lacabanne C. DC and AC conductivity of carbon nanotubes-polyepoxy composites. Macromolecules. 2003;36(14):5187-94.
[45] Jonscher AK. The "universal" dielectric response. Nature. 1977;267:673-9.
[46] Kymakis E, Amaratunga GA. Electrical properties of single-wall carbon nanotube-polymer composite films. Journal of Applied Physics. 2006;99(8):084302--7.
[47] Gorrasi G, Sarno M, Di Bartolomeo A, Sannino D, Ciambelli P, Vittoria V. Incorporation of carbon nanotubes into polyethylene by high energy ball milling: morphology and physical properties. Journal of Polymer Science Part B: Polymer Physics. 2007;45(5):597-606.
[48] De Vivo B, Guadagno L, Lamberti P, Raimo R, Sarto M, Tamburrano A, et al. Electromagnetic properties of carbon nanotube/epoxy nanocomposites. Electromagnetic Compatibility-EMC Europe, 2009 International Symposium on: IEEE; 2009. p. 1-4.
[49] Shui X, Chung D. A piezoresistive carbon filament polymer-matrix composite strain sensor. Smart Materials and Structures. 1996;5(2):243.
[50] Simmons JG. Generalized formula for the electric tunnel effect between similar electrodes separated by a thin insulating film. Journal of Applied Physics. 1963;34:1793.
[51] Sheng P, Sichel E, Gittleman J. Fluctuation-induced tunneling conduction in carbon-polyvinylchloride composites. Physical Review Letters. 1978;40(18):1197.
[52] Aneli JN, Zaikov GE, Khananashvili LM. Effects of mechanical deformations on the structurization and electric conductivity of electric conducting polymer composites. Journal of applied polymer science. 1999;74(3):601-21.
[53] Das NC, Chaki TK, Khastgir D. Effect of axial stretching on electrical resistivity of short carbon fibre and carbon black filled conductive rubber composites. Polymer international. 2002;51(2):156-63.
[54] Knite M, Teteris V, Kiploka A, Kaupuzs J. Polyisoprene-carbon black nanocomposites as tensile strain and pressure sensor materials. Sensors and Actuators A: Physical. 2004;110(1):142-9.
[55] Wang S, Chung D. Electrical behavior of carbon fiber polymer-matrix composites in the through-thickness direction. Journal of materials science. 2000;35(1):91-100.

[56] Gordon DA, Wang S, Chung D. Piezoresistivity in unidirectional continuous carbon fiber polymer-matrix composites: single-lamina composite versus two-lamina composite. Composite Interfaces. 2004;11(1):95-103.
[57] Njuguna M, Yan C, Hu N, Bell J, Yarlagadda P. Sandwiched carbon nanotube film as strain sensor. Composites Part B: Engineering. 2012;43(6):2711-7.
[58] Park M, Kim H, Youngblood JP. Strain-dependent electrical resistance of multi-walled carbon nanotube/polymer composite films. Nanotechnology. 2008;19(5):055705.
[59] Wichmann MH, Buschhorn ST, Gehrmann J, Schulte K. Piezoresistive response of epoxy composites with carbon nanoparticles under tensile load. Physical Review B. 2009;80(24):245437.
[60] Yasuoka T, Shimamura Y, Todoroki A. Electrical resistance change under strain of CNF/flexible-epoxy composite. Advanced Composite Materials. 2010;19(2):123-38.
[61] Yin G, Hu N, Karube Y, Liu Y, Li Y, Fukunaga H. A carbon nanotube/polymer strain sensor with linear and anti-symmetric piezoresistivity. Journal of Composite Materials. 2011;45(12):1315-23.
[62] Shimamura Y, Kageyama K, Tohgo K, Fujii T. Cyclic behavior of electrical resistance type low stiffness, large strain sensor by using carbon nanofiber/flexible epoxy composite. Key Engineering Materials. 2011;462:1200-5.
[63] Hu N, Fukunaga H, Atobe S, Liu Y, Li J. Piezoresistive strain sensors made from carbon nanotubes based polymer nanocomposites. Sensors. 2011;11(11):10691-723.
[64] Guadagno L, Raimondo M, Naddeo C, Di Bartolomeo A, Lafdi K. Influence of multiwall carbon nanotubes on morphological and structural changes during UV irradiation of syndiotactic polypropylene films. Journal of Polymer Science Part B: Polymer Physics. 2012;50(14):963-75.
[65] Böger L, Wichmann MH, Meyer LO, Schulte K. Load and health monitoring in glass fibre reinforced composites with an electrically conductive nanocomposite epoxy matrix. Composites Science and Technology. 2008;68(7):1886-94.

Table 1 - Prepared samples

Sample	CNT [% wt/wt]	CNT volume fraction [/]
Epoxy-0.015CNT	0.015	8.88×10^{-5}
Epoxy-0.025CNT	0.025	1.48×10^{-4}
Epoxy-0.05CNT	0.05	2.96×10^{-4}
Epoxy-0.1CNT	0.1	5.92×10^{-4}
Epoxy-0.3CNT	0.3	1.78×10^{-3}
Epoxy-0.5CNT	0.5	2.97×10^{-3}
Epoxy-1.0CNT	1.0	5.94×10^{-3}

Figure 1

Click here to download high resolution image

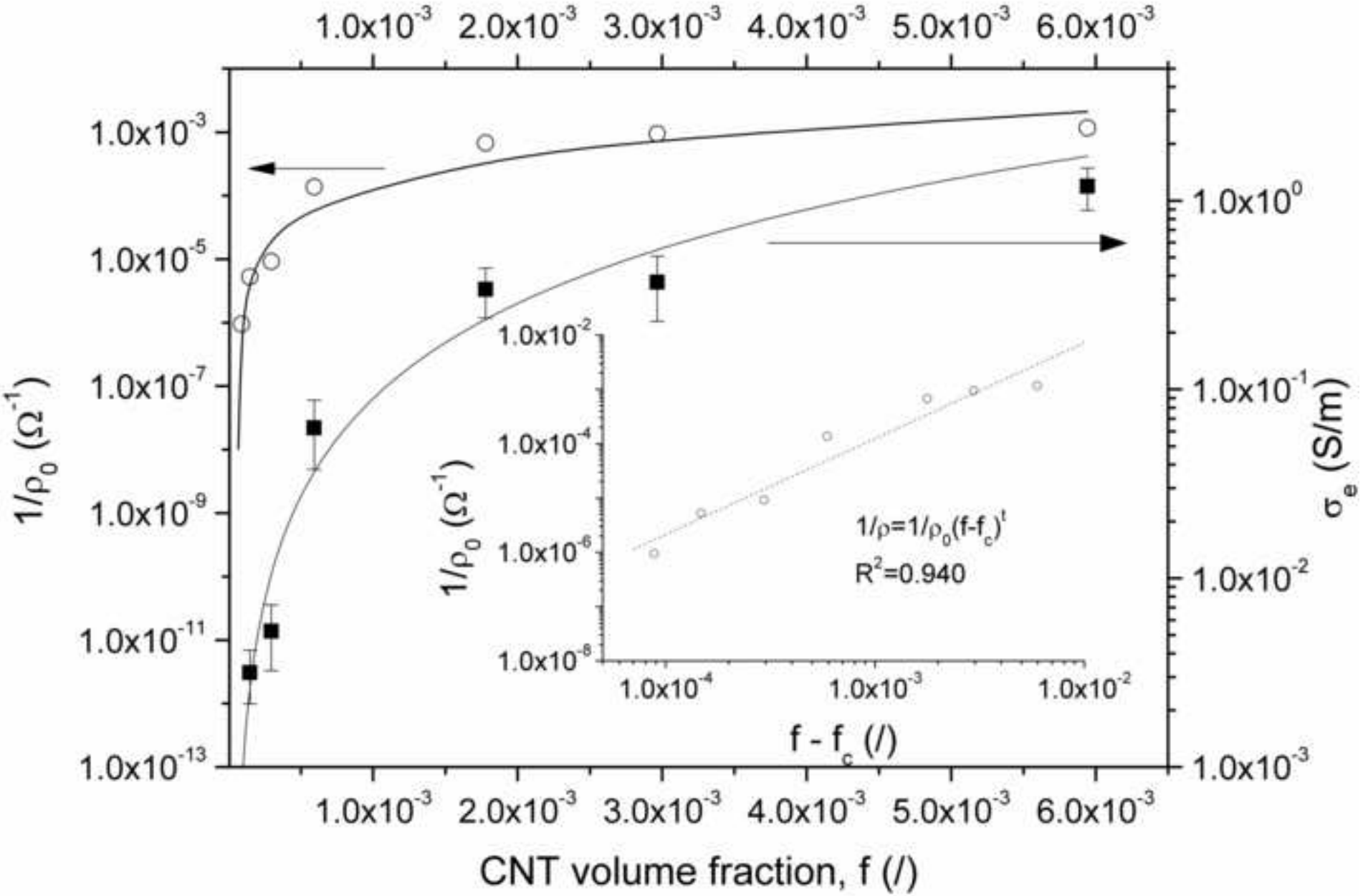

Figure 2

Click here to download high resolution image

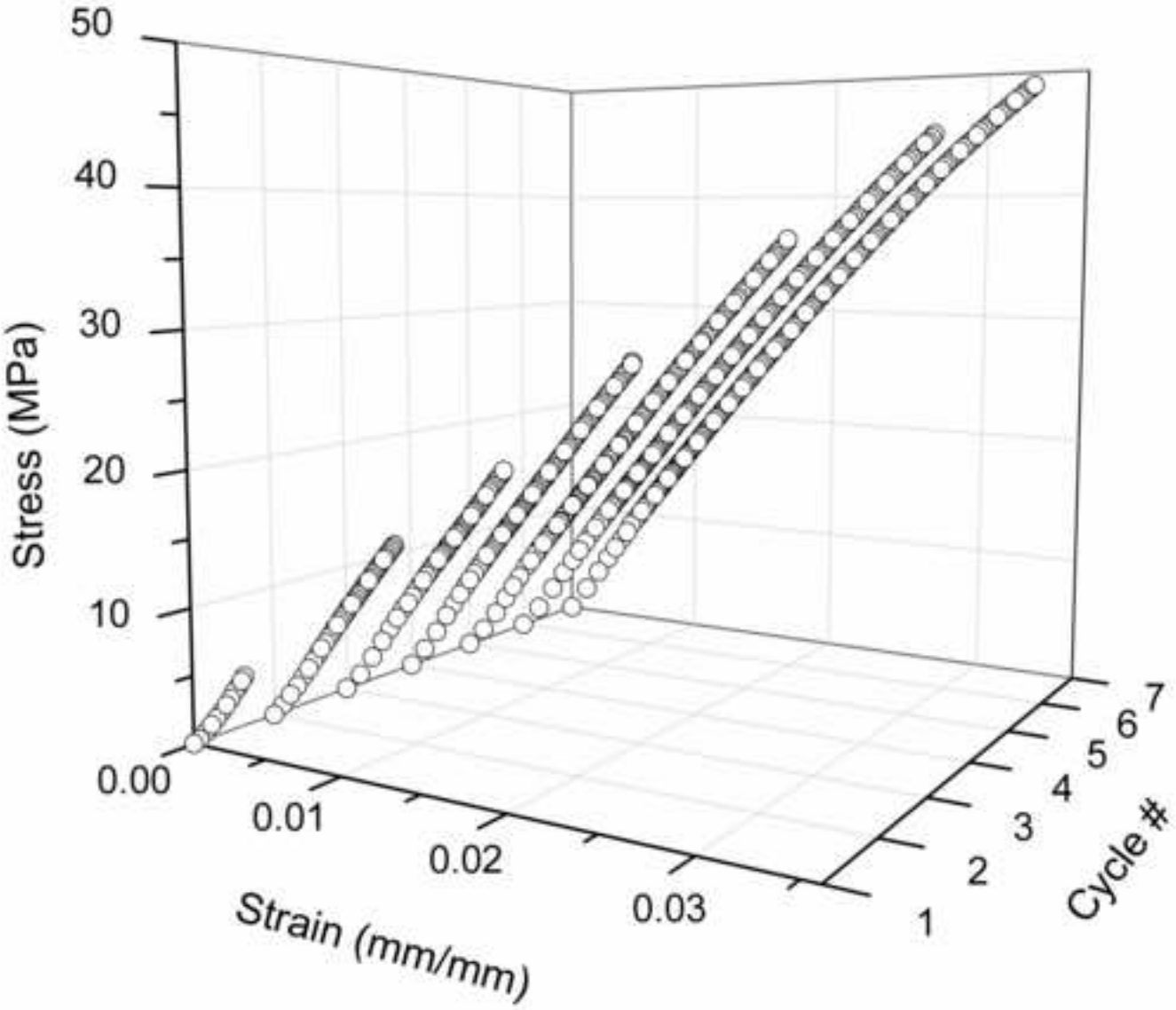

Figure 3

Click here to download high resolution image

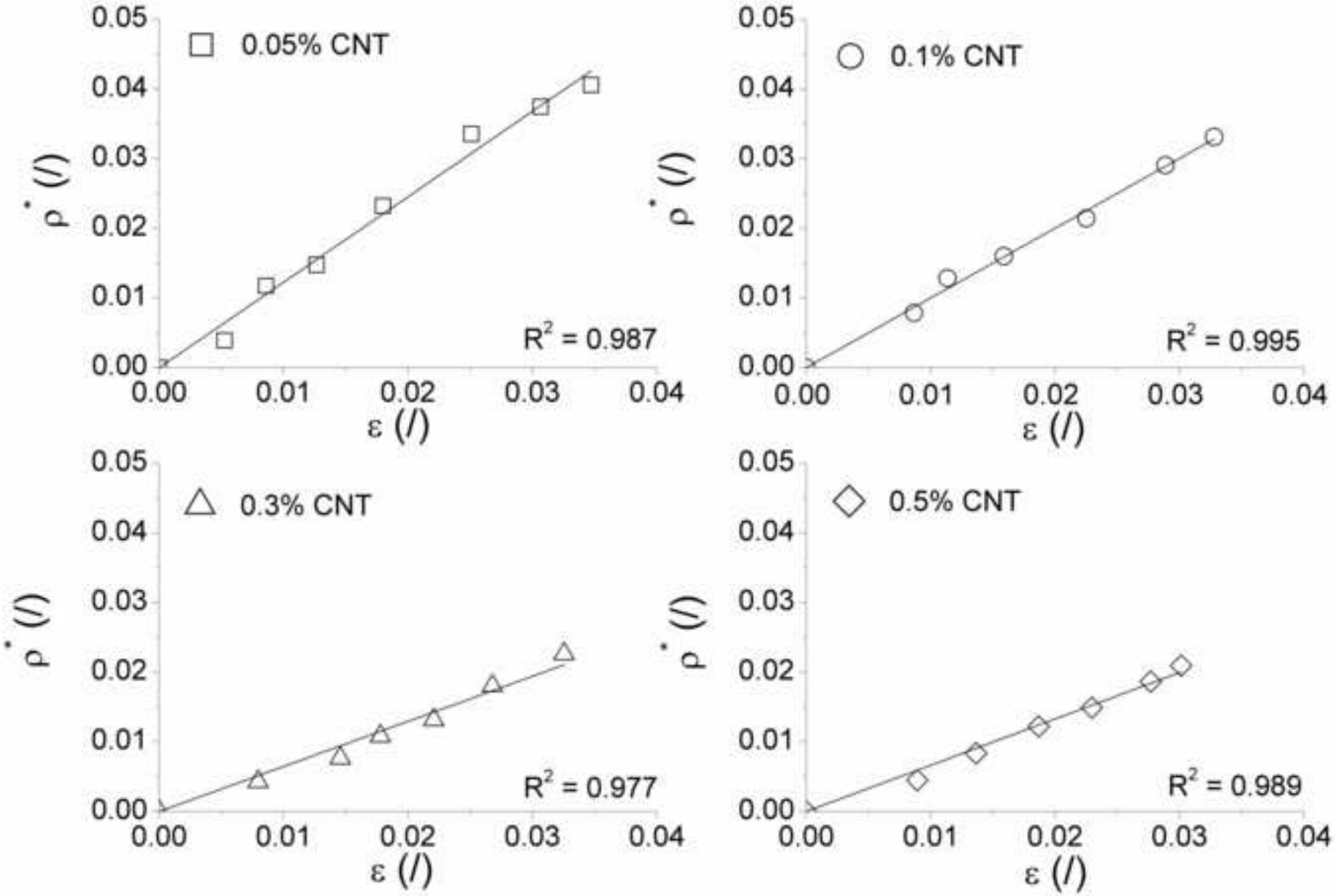

Figure 4

Click here to download high resolution image

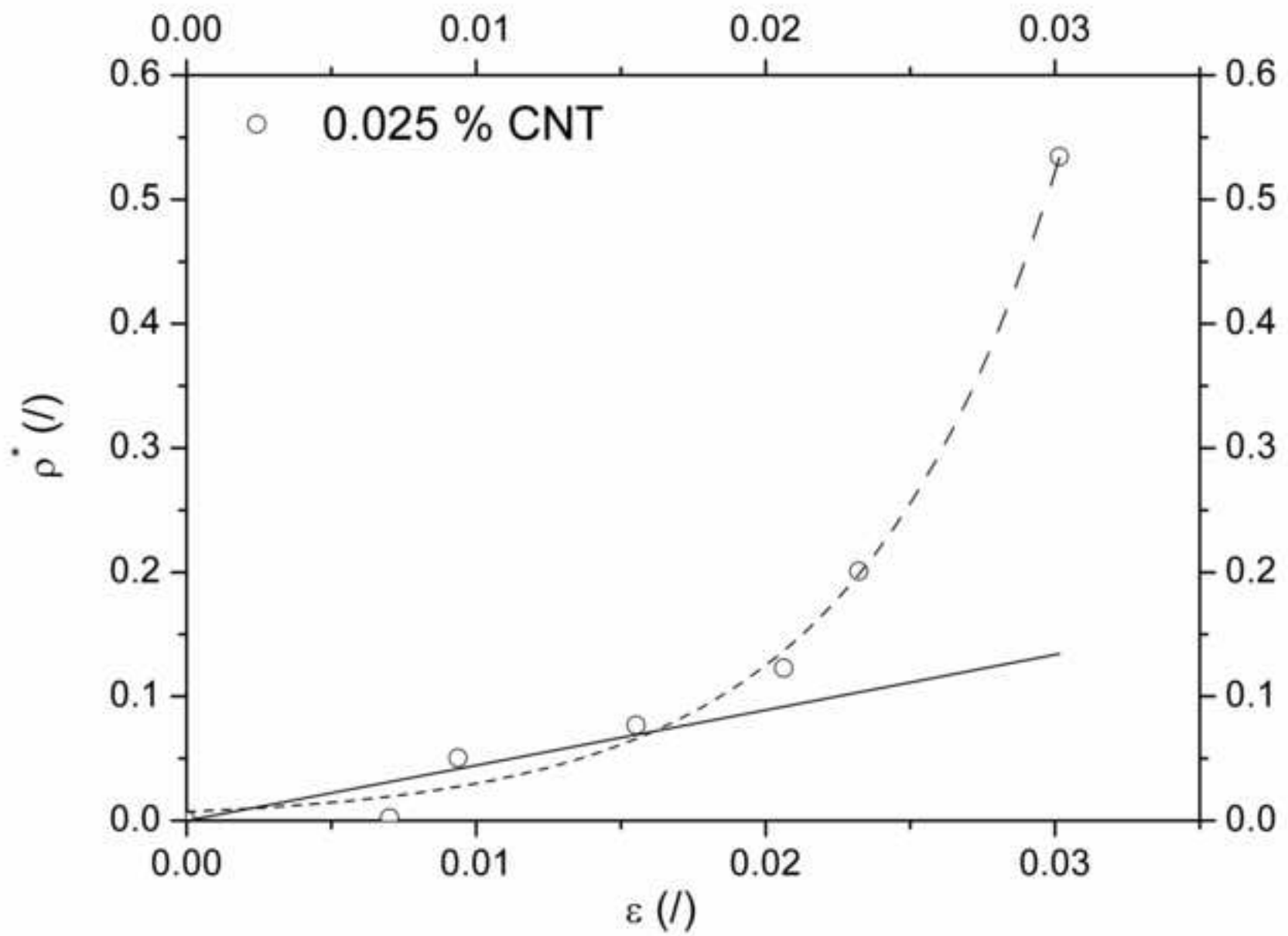

Figure 5

Click here to download high resolution image

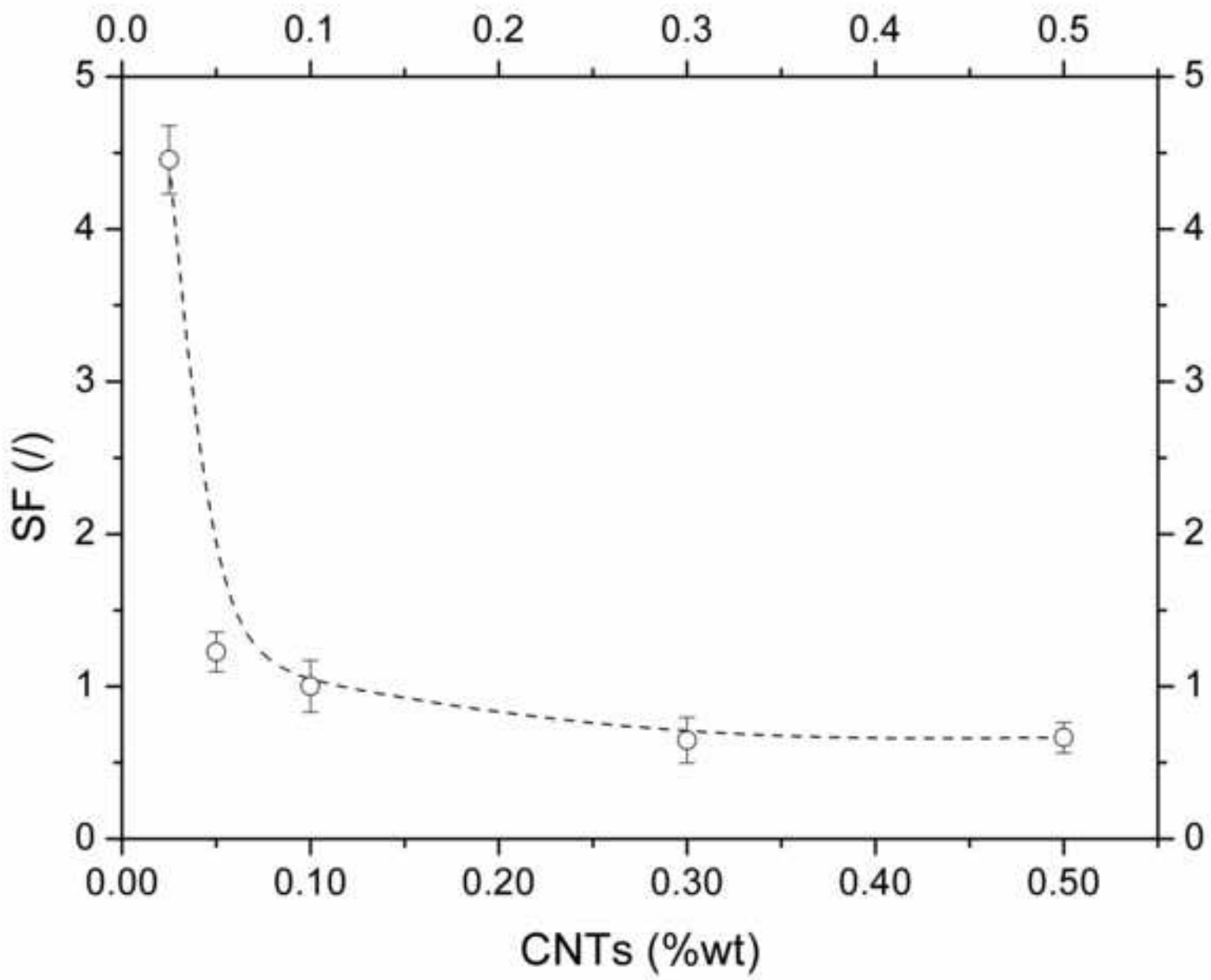

Figure 6
Click here to download high resolution image

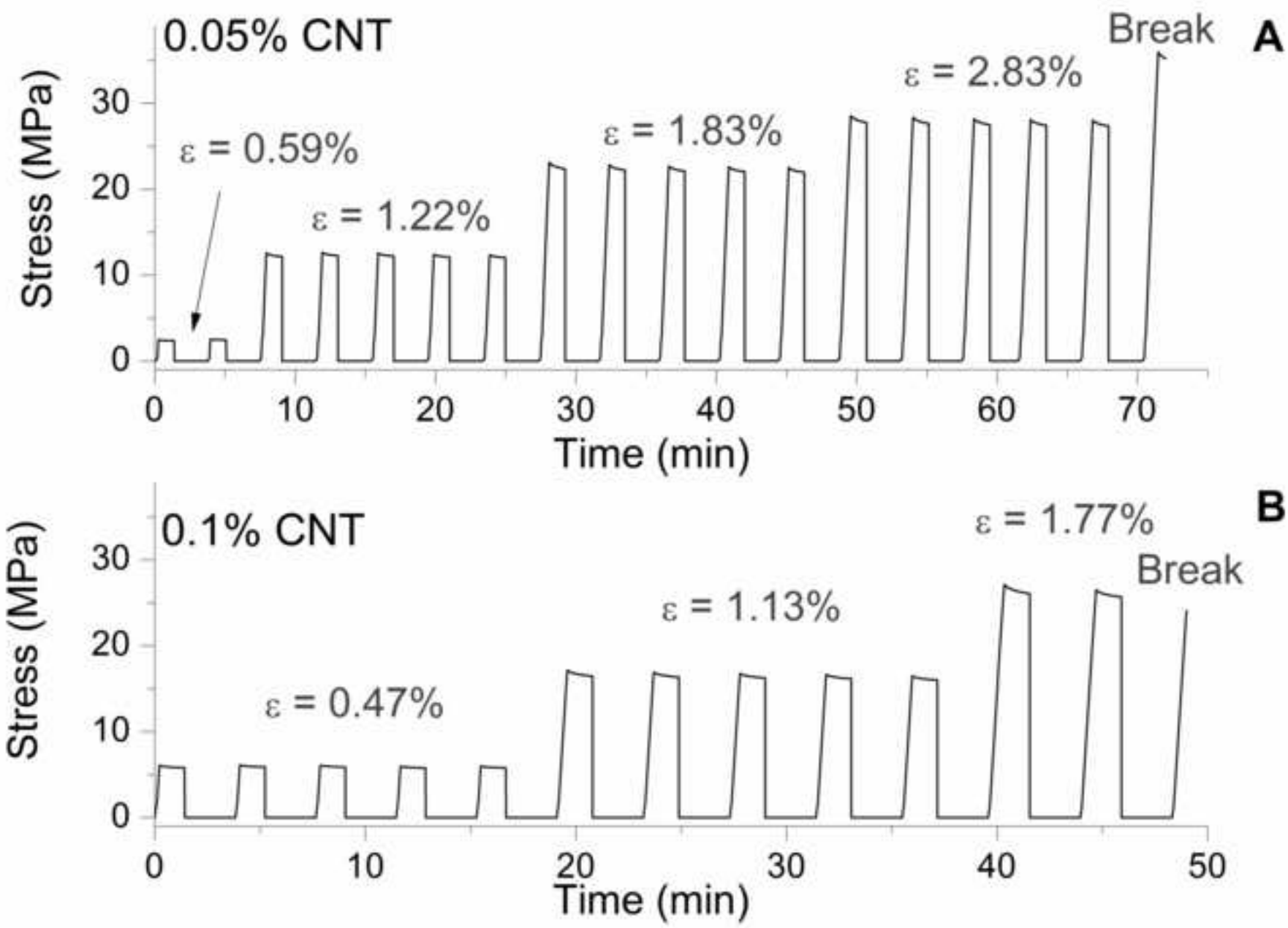

Figure 7

Click here to download high resolution image

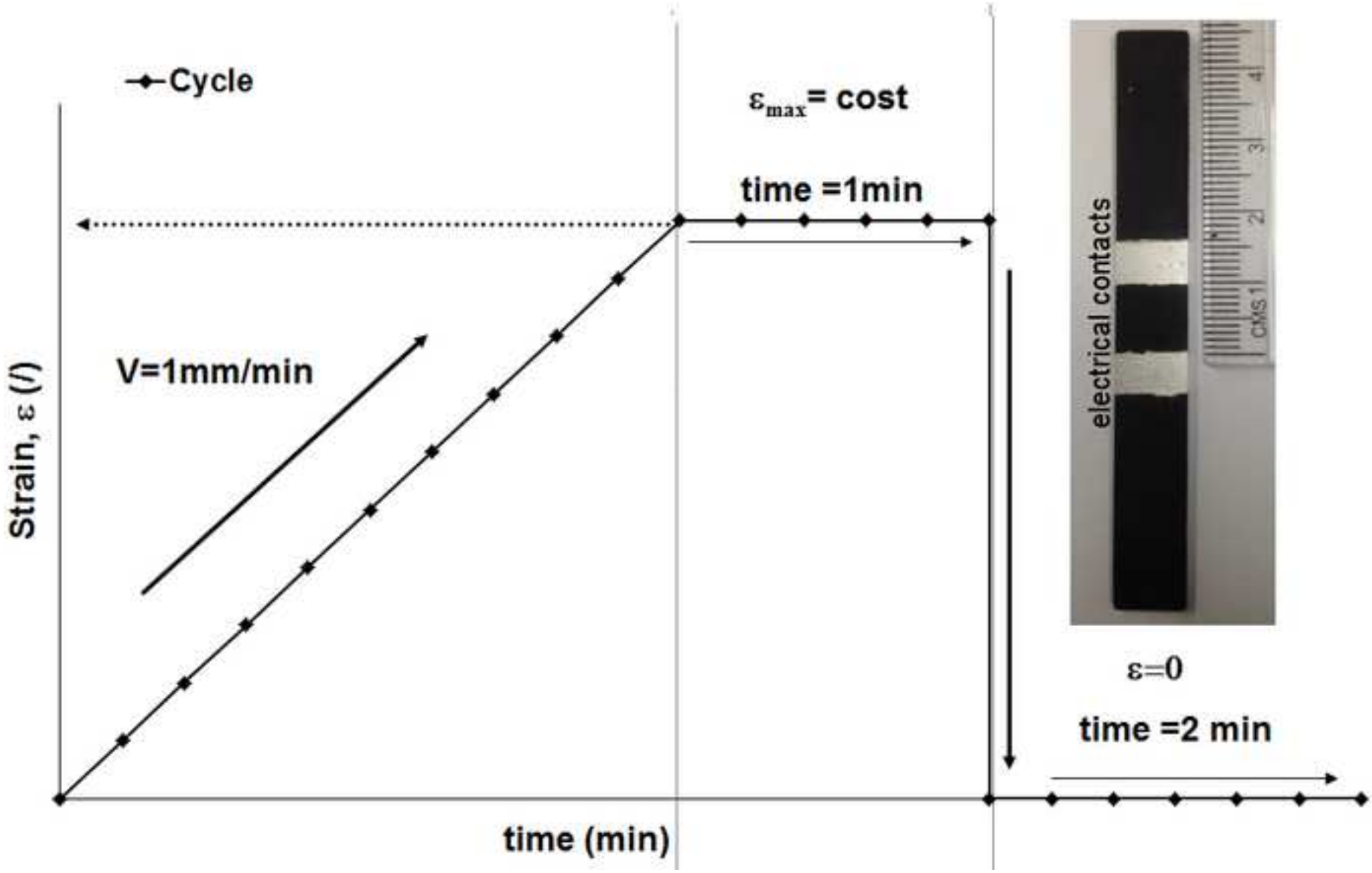

Figure 8
Click here to download high resolution image

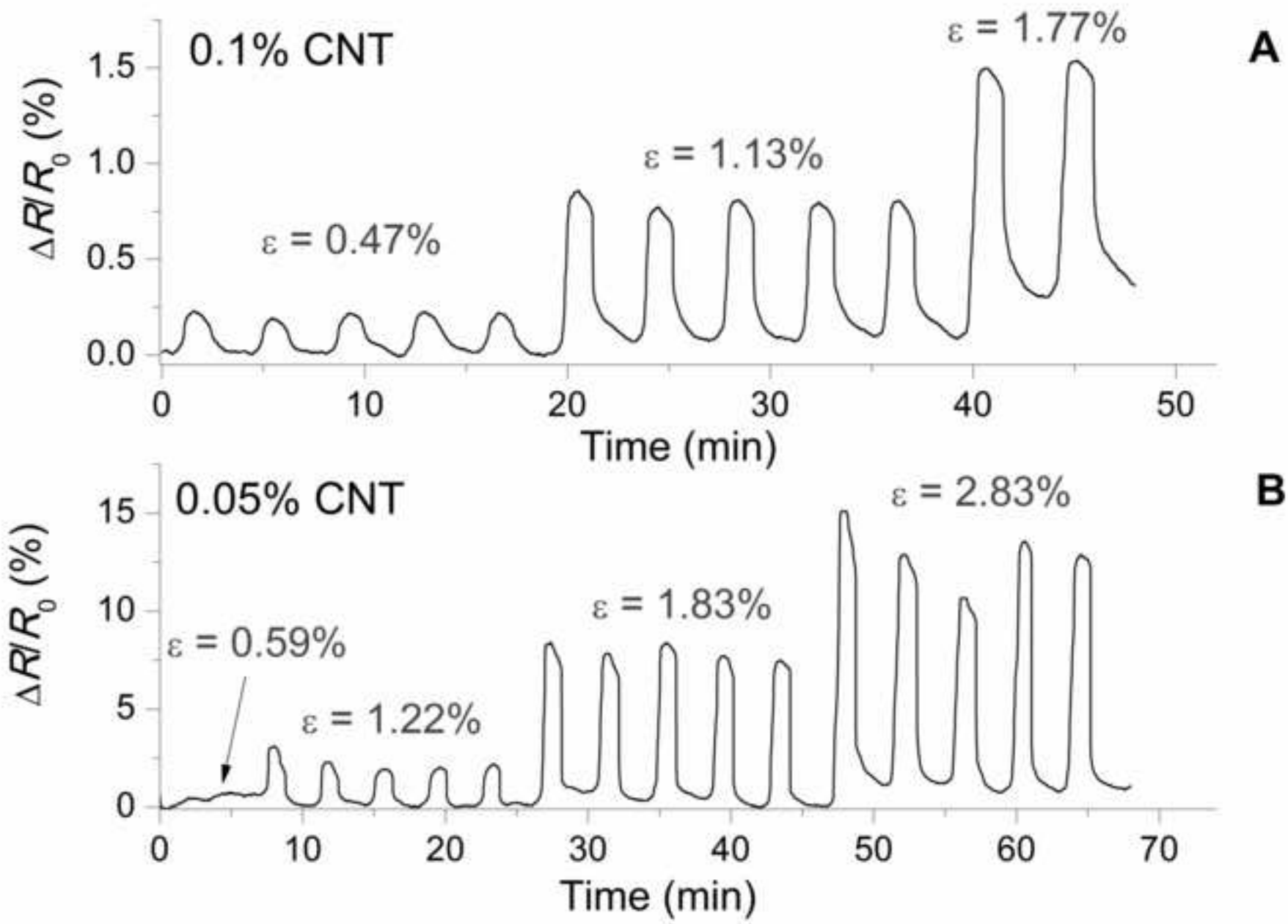

Figure 9

Click here to download high resolution image

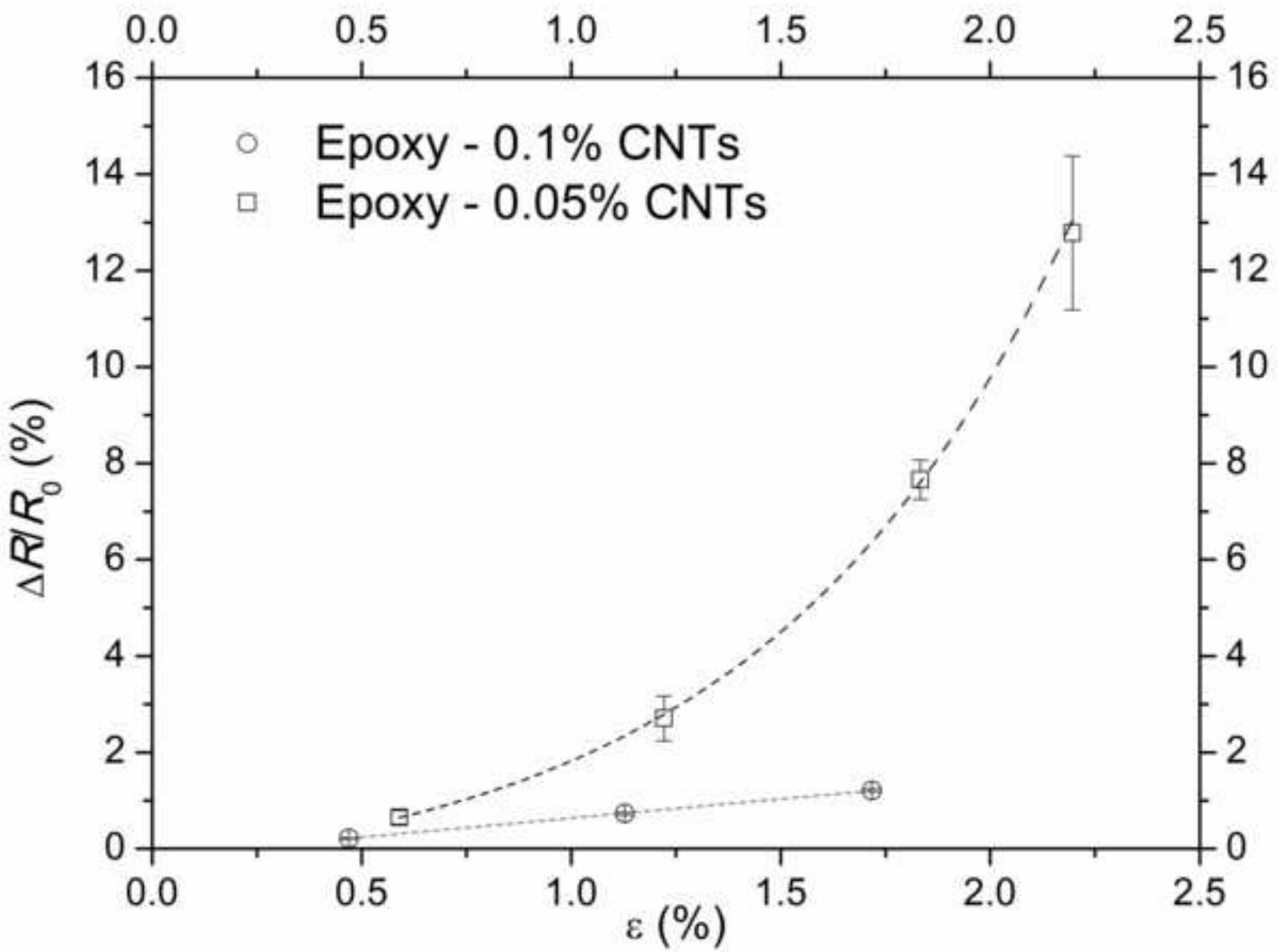

List of Figure Captions

Fig. 1. Inverse of surface resistivity, $1/\rho_0$ on the left axis, before the mechanical tests and without any load applied and volume electrical conductivity, σ_e on the right axis, vs CNT volume fraction.

Fig. 2. Stress-strain behavior cycles for sample containing 0.1% wt/wt of CNTs.

Fig. 3. Behavior of normalized surface resistivity vs strain for samples in the range 0.05÷0.5% wt/wt.

Fig. 4. Behavior of normalized surface resistivity vs strain for the sample Epoxy-0.025CNT.

Fig. 5. Comparison of sensitivity factors for different weight percentage of CNTs.

Fig. 6. Temporal behavior of tensile stress for samples containing: (A) 0.05% wt/wt CNTs; (B) 0.1% wt/wt CNTs.

Fig. 7. The schematic diagram of single cycle in tensile test, and sample photo before testing.

Fig. 8. The change in electrical resistance in tensile test for samples containing: (A) 0.1% wt/wt CNTs; (B) 0.05% wt/wt CNTs.

Fig. 9. The change in electrical resistance vs strain for samples containing 0.1% wt/wt and 0.05% wt/wt CNTs.

List of Table Captions

Table 1 - Prepared samples